EFFECTS OF HIGH-ENERGY BALL MILLING ON STRUCTURE AND MECHANICAL PROPERTIES OF $L1_2$ INTERMETALLIC COMPOUND $Al_{67}Mn_8Ti_{25}$ ①

Fu Yunyi, Wan Qian and Hu Gengxiang
The Education Ministry of China Open Research Lab for High Temperature Materials and Testing, Shanghai Jiao Tong University, Shanghai 200030, P. R. China

ABSTRACT $Al_{67}Mn_8Ti_{25}$ powder was produced by high-energy ball milling and then consolidated by vacuum hot pressing and hot isostatic pressing. The effects of mechanical milling on the structure and properties of the alloy had been investigated. The results show that the long range order parameter of $L1_2$ structure decreased rapidly in the early stage of milling. After 5 h milling, the material is completely disordered, forming a FCC solid solution. By further milling to 60 h, the powder transformed to purely amorphous state. Bulk specimens were fabricated from the disorder FCC powder by hot pressing at high temperature. The microstructure of the consolidated alloy consists of fine equiaxed grains with tiny particles of dispersed Al_2O_3 at grain boundaries and in the grains. Remarkable improvement of strength and promising compressive ductility are exhibited by this experimental alloy. The yield strength ($\sigma_{0.2}$) and fracture strength (σ_b) are 546 MPa and 1 471 MPa respectively, and the compressive ductility (δ_p) is 17%.

Key words $Al_{67}Mn_8Ti_{25}$ alloy high-energy ball milling powder metallurgy structure evolution intermetallic compound

1 INTRODUCTION

The ordered intermetallic compound Al_3Ti is noticeable because of its low density (3.4 g/cm^3), excellent high-temperature oxidation resistance (~ 1 200 ℃), high modulus and good strength at elevated temperatures. Although Al_3Ti is potentially a light-weight high-temperature material, it is necessary to overcome its room-temperature brittleness for satisfying the demand of industrial applications. In recent years, efforts had been made to change the low symmetry DO_{22} structure of Al_3Ti into the cubic $L1_2$ structure by alloying with Mn, Cr, Fe and so on, so as to improve the mechanical behavior of Al_3Ti compound. However, the room-temperature ductility of the $L1_2$ type Al_3Ti alloy is improved only a little while the yield strength is still rather low[1-3]. In the present work, high-energy ball milling was used to explore a new approach for the srengthening and toughening of the $L1_2$ Al_3Ti alloy. The effects of mechanical milling on the structure and property of the Al_3Ti alloy were investigated.

2 EXPERIMENTAL

The vacuum induction melted intermetallic alloy $Al_{67}Mn_8Ti_{25}$ ingot was mechanically powdered prior to milling. The milling was performed with a high-energy ball mill QM-1SP. Both the vial and balls are made of GCr15 bearing steel. The ball-to-powder mass ratio was 60∶1. An addition of 1% stearic acid was used

① Project 59771005 supported by the National Natural Science Foundation of China, the Doctoral Education Foundation of Education Ministry of China and the National Key Lab of Powder Metallurgy at Central South University of Technology
Received Sep. 1, 1997; accepted Mar. 23, 1998

to eliminate agglomerate during the milling process. The alloy powder was then consolidated by CIPping (280 MPa), vacuum sintering (960 ℃, 1 h), vacuum hot pressing (1 120 ℃, 20 MPa, 1 h) and HIPping (1 120 ℃, 130 MPa, 2 h) sequentially. For structural characterization, a Rigaku D-Max/ ⅢA X-ray diffractometer was used. Compression tests were made with the 4 mm × 4 mm × 7 mm specimens spark-erode from the HIPped blocks, the starting strain rate for testings was $2.4 \times 10^{-4} s^{-1}$. The morphology of fractured surface was examined by a scanning electron microscope S-520. TEM analysis was conducted on the JEM 100CX electron microscope.

3 RESULTS AND DISCUSSION

3.1 Structural evolution during high-energy milling

The refinement of $Al_{67}Mn_8Ti_{25}$ powder during the milling process was prominent. SEM measurements determined that the granular size was 5~ 10 μm after 1 h milling (Fig. 1a), and reduced to 2~ 3 μm on an average after 5 h milling (Fig. 1b). The effect of high-energy ball milling on the crystal structure of the $Al_{67}Mn_8Ti_{25}$ alloy was studied by X-ray diffraction method. Fig. 2 shows the XRD patterns of the alloy after different milling times. The equilibrium state of the $Al_{67}Mn_8Ti_{25}$ alloy before milling exhibited the ordered cubic $L1_2$ structure (Fig. 2a). At the early stage of milling, the intensities of $L1_2$ superlattice reflections decreased markedly (Fig. 2b), indicating the diminishment of ordering. The superlattice peaks completely disappeared after 5 h milling, only FCC diffraction peaks remained but their profiles were broadened (Fig. 2c). This means that the alloy structure had been changed from the ordered $L1_2$ into the disordered FCC structure. Extending the milling time, the FCC diffraction peaks broadened further and their intensities were weaker and weaker (Figs. 2d, e). Finally the diffraction pattern changed into a diffuse diffraction halo at $2\theta = 34° \sim 50°$, indicating the alloy had been transformed into the amorphous state. To compare the asymmetrical broadening of (111) diffraction peak in Figs. 2c~ e with the diffuse halo in Fig. 2f, it can be realized that the amorphous transformation during the milling was a gradual process. The alloy powder after 60 h milling had been inspected by TEM, its TEM image and electron diffraction pattern were characterized as the amorphous state (Fig. 3) which confirms the XRD result.

The variation of long-range order parameter S of the $L1_2$ structure during milling can be

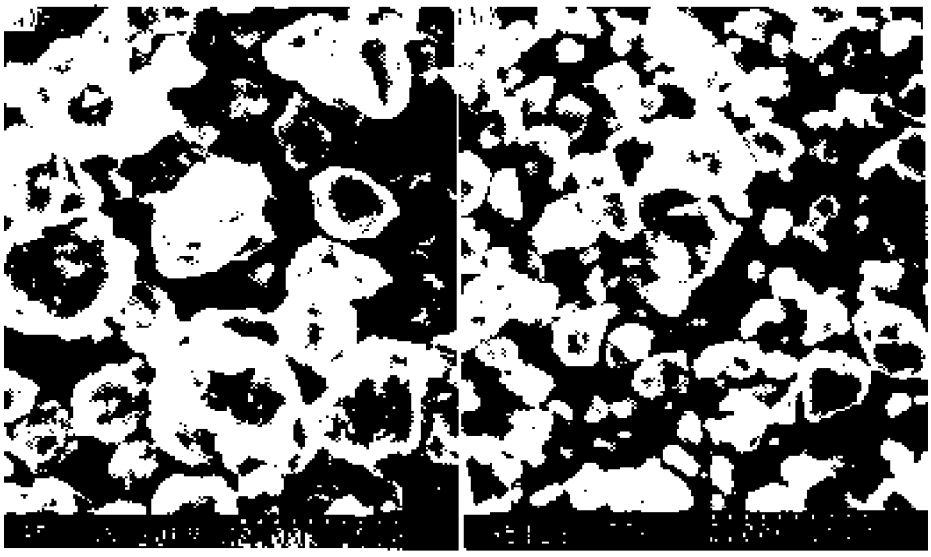

Fig. 1 Particle morphology of $Al_{67}Mn_8Ti_{25}$ alloy after 1 h (a) and 5 h (b) high-energy ball milling

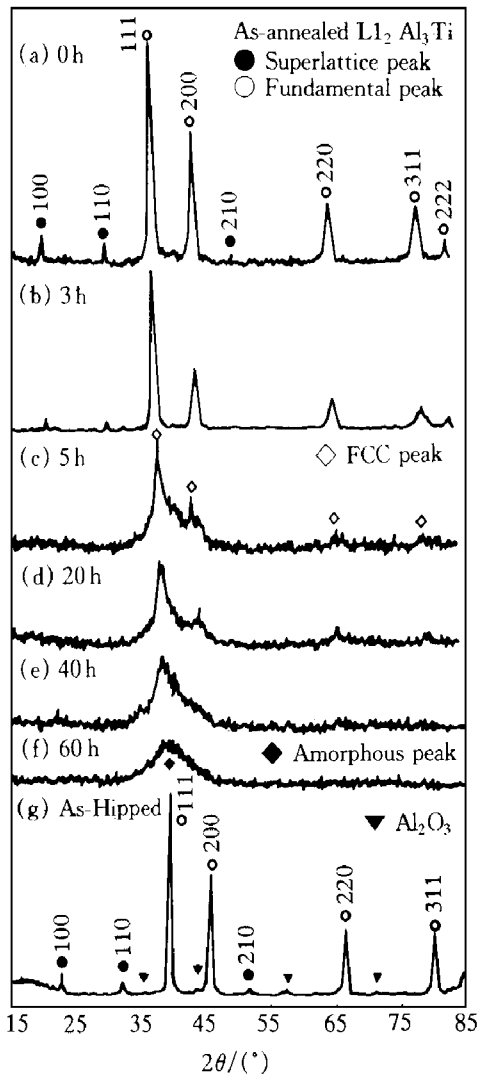

Fig. 2 XRD spectra of $Al_{67}Mn_8Ti_{25}$ under different conditions

Fig. 3 TEM micrograph and EDP of $Al_{67}Mn_8Ti_{25}$ after 60 h milling

determined from the XRD spectra after different milling times. The S value is calculated by[4]:

$$S^2 = \frac{I_s}{I_f} \cdot \frac{f_{Al} + 3f_{Ti}}{f_{Ti} - f_{Al}} \cdot \frac{L_F \cdot D_F}{L_s \cdot D_s}$$

where I_s and I_f are intensities of superlattice diffraction and fundamental diffraction respectively, here the (110) superlattice peak and (220) fundamental peak were chosen for measurements; f_{Al} and f_{Ti} are atomic scattering factors of Al and Ti, while the influence of Mn atom had been neglected for simplifying the calculation; L_s, L_F and D_s, D_F are Lorentz factor and Debye factor of the superlattice and fundamental diffraction, respectively. The results are shown in Fig. 4; it can be seen that the degree of order quickly decreases to zero after 5 h ball milling, while further milling leads to amorphous transition.

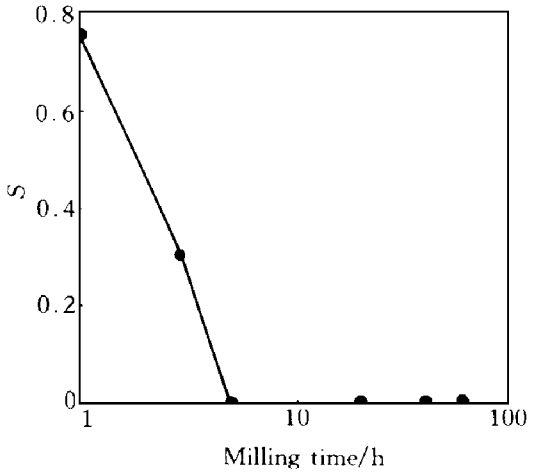

Fig. 4 Changes of long-range order parameter S during milling

The formation of metastable FCC structure or amorphous phase must satisfy the thermodynamic principle, i.e. the free energy of the system must be raised to the value for such kind of non-equilibrium transformation to take place. During the high-energy ball-milling process, the $Al_{67}Mn_8Ti_{25}$ powder suffered severe crushing, cold-welding, deforming and fracturing, which induced a huge amount of lattice defects, internal strain and interfaces which accumulated in the alloy powder, thus the free-energy of the system increased significantly. To demonstrate the above mentioned effects of milling process,

the changes of internal strain and grain size had been determined separately from the broadening of diffraction peaks during milling by the method suggested by Williamson-Hall[5]. The results are shown in Fig. 5; it is found that the grain size reduced quickly even at the early stage of milling, thus the amount of grain boundary greatly increased, in the meanwhile the internal strain of the powder also rose significantly. All such evidences resulted in the rise of total free energy. The disordered FCC structure formed at the early stage of milling is a highly supersaturated solid solution with low lattice stability. When the subsequent milling further increased the free energy which became higher than the free energy of the amorphous state, the FCC structure would transform into the amorphous phase.

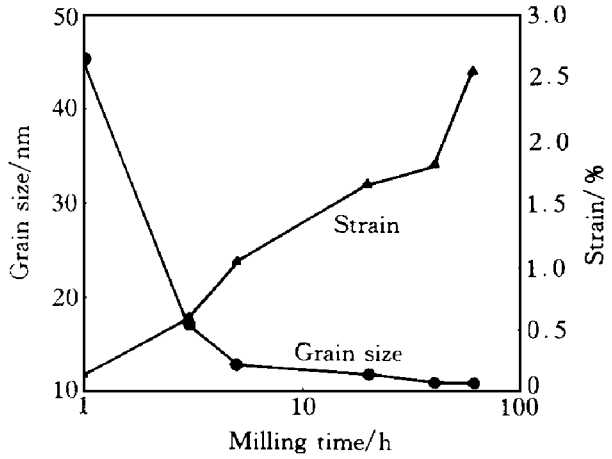

Fig. 5 Changes of grain size(a) and internal strain(b) during milling

3.2 Structure and property of high-energy ball milled alloy

The above experiments showed that the $L1_2$ structure of $Al_{67}Mn_8Ti_{25}$ alloy can be changed into a disordered FCC state after 5 h high-energy ball milling, while 60 h milling is necessary for the completely amorphous transition. On practical consideration, we first studied the influence of FCC state powder on the microstructure and property of the consolidated $Al_{67}Mn_8Ti_{25}$ intermetallic alloy.

The 6 h milled FCC metastable powders were consolidated by means of the above mentioned powder metallurgy fabrication method. The microstructure of the bulk material is shown in Fig. 6, which is composed of equiaxed fine grains with the size of 2~ 10μm, illustrating the occurrence of recrystallization during high temperature XRD analysis determined that the alloy had returned to its equilibrium $L1_2$ structure (Fig. 2g). It can be observed also in the micrograph that there are many fine particles distributed along grain boundaries and in the grains. It is also found in the XRD spectra some small diffraction peaks other than the $L1_2$ peaks which are identified as Al_2O_3. These fine Al_2O_3 particles are supposed to be formed during the ball milling process.

Fig. 6 Microstructure of HIPped $Al_{67}Mn_8Ti_{25}$

The room-temperature mechanical property of the powder-fabricated $Al_{67}Mn_8Ti_{25}$ alloy is listed in Table 1, the properties of the vacuum induction melted ingot specimens (after homogenization-annealing) and the hot-worked specimens (after recrystallization annealing) are also listed for comparison[6]. It can be seen that the strength and ductility of the cast alloy are rather low and hot-working improves the mechanical properties to a certain extent, while the alloy made of high-energy ball milled powder behaves much higher strength and good ductility.

The microstructural features of the powder-

fabricated alloy indicate that the strengthening effects are mainly due to the grain refinement and the dispersed particles. The extra-fine grains formed by high-energy milling can still maintain small grain microstructure after high temperature sintering and HIPping. This is due to the severe internal strain caused by milling which leads to a very high nucleation rate of recrystallization, and the growth of grains is impeded by the dispersed fine particles. These oxide particles formed during the milling process not only serve as the barriers for grain growth, but also give rise to the strengthening effect by hindering the motion of dislocations and arresting the propagation of micro-cracks. Fig. 7 shows the SEM fractograph

Fig. 7 SEM fractograph of HIPped $Al_{67}Mn_8Ti_{25}$

of the powder-fabricated $Al_{67}Mn_8Ti_{25}$ specimen after fractured by compression testing, its morphorlogy is different from the cleavage fractography of conventional cast or hot-worked specimen[7]. This fracture surface composed of finely mixed intergranular and transgranular fractures with some evidence of plastic deformation. The tortuous feature of the crack path illustrates that the propagation of cracks has met many obstacles, so that the mechanism of strengthening and toughening effects can be demonstrated.

Previous studies had concluded that the $L1_2$ structured Al_3Ti alloy is still brittle at ambient temperature and behaves low strength level. Since the $L1_2$ structure exists only in a narrow compositional range of the Al-Ti-X tenary system[8], it is difficult to improve the mechanical properties by further alloying in the single phase region. The present work provides a new approach for the strengthening and toughening of Al_3Ti alloy. The results reported in this paper have demonstrated the potentiality of this approach, further improvement of the mechanical properties is possible through the optimizing of process and control of microstructure.

Table 1 Room-temperature compression properties of $Al_{67}Mn_8Ti_{25}$ alloys

Condition of specimen	$\sigma_{0.2}$/ MPa	σ_b/ MPa	δ_p/ %
Cast+ homogenizing	218	512	12.5
Hot-worked+ recrystallizing-annealed	248	980	18.0
High-energy ball-milled powder consolidated	546	1471	17.0

REFERENCES

1 Inui H, Luzzi D E, Porter W D *et al*. Phil Mag, 1992, A 65(1): 245.
2 Brown S A and Kumar K S. Scr Metall Mater, 1990, 24: 2001.
3 Hu G, Chen S, Wu X *et al*. J Mater Res, 1991, 6 (5): 957.
4 Morris D G. Metall Mater Trans A, 1994, 25: 449.
5 Williamson G K and Hall W H. Acta Metall, 1953, 1: 22.
6 Chen X, Chen S, Wu X *et al*. Mater Sci Eng, 1992, A 153: 37.
7 Lerf R and Morris D G. Acta Metall, 1991, 39: 2419.
8 Murray J L. Phase Diagrams of Binary Titanium Alloys. Metals Park, OH: ASM International, 1987: 22- 24.

(Edited by Peng Chaoqun)